Thin elastic plates: On the core of developable cones

T. MORA[1] and A. BOUDAOUD[1,2](*)

[1] *Laboratoire de Physique Statistique de l'ENS*
24, rue Lhomond, 75231 Paris Cedex 05, France
[2] *MIT, Department of Mathematics - 77 Massachusetts Avenue*
Cambridge MA 02139-4307, USA

Abstract. – Large deformations of thin elastic plates lead generally to the focusing of deformations around almost singular structures which are either linear (curved and straight ridges) or point-like (developable cones), as can be observed for crumpled paper. An experiment has been devised to study the core of a developable cone. An initially bent plate is loaded at its center. It is either drilled with two holes or made of metal. The experimental results are used to measure the energy of the core for both elastic and plastic deformations. It is shown that the behaviour of a plate when plastic deformations occur, as in practical applications, can be deduced from its behaviour when deformations are perfectly elastic. This result demonstrates that studies on large deformations of perfectly elastic plates may be used for applications.

Introduction. – Thin elastic structures are of huge practical and industrial importance. Examples range from cans to planes, including all sorts of containers, ships, rockets, ... This importance has motivated a large number of studies on the stability of these structures (see [1] for the case of cylinders): if they are constrained, they loose their shape (they buckle) at a critical force. Of course, one would like to increase this buckling threshold for applications. The buckling of thin plates has also been investigated as a model for pattern formation [2]. Microscopic membranes such as polymer networks [3], solid Langmuir monolayers [4] or actin-coated membranes [5] buckle when compressed. These sheets are similar to biological membranes such as blood red-cell membranes [6]. This similarity has stimulated many theoretical works on microscopic membranes [7]. At small scales, thermal fluctuations are important: sheets are flat at low temperature and collapsed at high temperature. An intermediate crumpled phase has been predicted, but its observation is controversial [8]. Most theoretical macroscopic studies (see [1]) have been devoted to small deformations, as the complete equations are complicated. Large deformations of thin elastic plates are described by the Föppl-von Kármán equations [9], which are two fourth-order nonlinear coupled partial differential equations. Thus, analytical as well as numerical [10,11] resolutions are difficult. However, the existence of a small parameter, the ratio of the thickness h to a typical length R of the plate, allows asymptotic analysis. This field has grown recently and has aroused many experimental works [12–24]. When a thin plate is strongly constrained, deformations focus along almost singular lines (edges called ridges) which

---

(*) E-mail: `boudaoud@lps.ens.fr`

meet in points (vertices called developable cones), as is easily observed with crumpled paper. In this letter, we are concerned with point-like singularities. As far as we are aware, we give the first measurement and modeling of their core energy for both elastic and plastic deformations.

Thin elastic plates have two modes of deformation, bending and stretching; their typical elastic energies are, respectively, [9] $E_{\mathrm{b}} \sim Eh^3 Z^2/R^2$ and $E_{\mathrm{s}} \sim Eh Z^4/R^2$, for a transverse displacement of magnitude Z, E being the elastic modulus of the material, h the plate thickness and R a typical length. It is much easier to bend a plate than to stretch it, as can be expected from the ratio $E_{\mathrm{s}}/E_{\mathrm{b}} \sim (Z/h)^2$, which is large as soon as the transverse deformation is larger than the plate thickness. So, pure bending deformations (with no stretching) are to be preferred. Then, the plate has the shape of a developable surface (one of its two curvatures is zero). However, there is not always a smooth developable surface satisfying the applied boundary conditions (the non-existence is in fact generic [16]). So, developable surfaces which are singular at curves or points are expected. Such developable surfaces also arise in the context of smectics [25]. Outside the singularities, there are pure bending deformations. When the plate thickness is finite, the singularities are smoothed, and the energetically expensive stretching is localized in boundary layers around the singularities of the developable surface. These singularities were mostly studied when they are isolated [12–20]. They have also been investigated in high dimensions [21]. In practice, plastic deformations occur first at the singularities where the strains are the larger (as shown for d-cones [19]).

Here we are concerned with point-like singularities (developable cones or d-cones). The sheet has locally the shape of a cone of angle ϕ (defined so that $\phi = 0$ if the cone is flat) and radius R. The tip of the cone is smoothed on a zone (the core) of radius R_{c}. The bending energy outside the core is given by [16]

$$E_{\mathrm{d}} = \kappa G \ln(R/R_{\mathrm{c}})\phi^2. \tag{1}$$

κ is the bending modulus

$$\kappa = \frac{Eh^3}{12(1-\nu^2)}, \tag{2}$$

ν being the Poisson ratio of the material. G is a geometric shape factor (material independent). G depends on the shape of the cone, but the value $G = 67$ computed for a single d-cone [17,18] has been shown to be quite general [24]. In situations with a few singularities, the energy of the plate is given by that of the d-cones [24]. Developable cones have been observed on fabrics [26], curved shells [22] and thin viscous sheets [27]. Two different scalings have been proposed for the size R_{c} of the core of a d-cone [16,18,20], the one consistent with experiments [19,20] is

$$R_{\mathrm{c}} = (\kappa/Eh)^{1/6} R^{2/3} \phi^{-1/3}, \tag{3}$$

for small tip angles. The energy of the core can be written as

$$E_{\mathrm{c}} = \kappa \gamma G \phi^2, \tag{4}$$

γ being another geometrical factor (material independent), which we expect to be as general as the value of G. The present experiment allowed us to measure γ although $E_{\mathrm{c}} < E_{\mathrm{d}}$ (which should make the measurement difficult). The principle is to drill holes in the plate so that a part of the d-cone core becomes virtual. Energies are measured by integrating the plate resisting force as a function of the imposed displacement. The energy difference between drilled and undrilled plates gives the core energy. Our second achievement was to model the behaviour of the plate when plastic deformations occur in the core.

The experiment. – A thin elastic plate of length $L = 35$ cm and width $W = 25$ cm is clamped on two sides and free on the other two sides. The distance d between the clamped
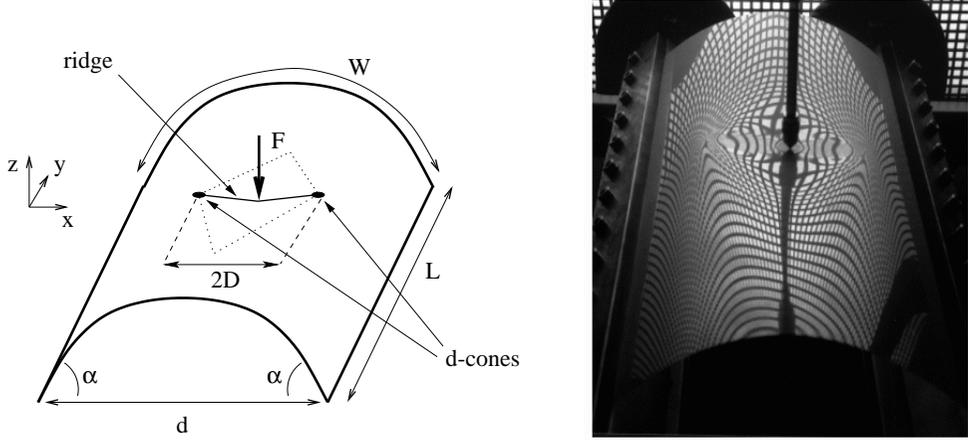
Fig. 1 – Sketch and photograph of the experiment. A rectangular plate clamped at two sides (at $x = \pm d/2$) has its centre pushed down. Two d-cones linked by a ridge of length $2D$ appear at small vertical displacement (here $Z = 5$ mm). The origin of axes is at the initial plate centre.

sides as well as their inclination angle α can be adjusted (fig. 1). A conical tip pushes the plate at its centre. The control parameter is the vertical displacement Z of the centre. A piezoelectric cell gives the plate resisting force F. Initially (when $Z = 0$), the plate is cylindrical, and we measure its curvature $2k$ at $x = 0$. As plates, we use: i) mylar sheets of thickness $h = 0.25$ mm, bending modulus $\kappa = 8.3 \cdot 10^{-3}$ N m and Poisson ratio $\nu = 0.4$ (as a reference case); ii) the same mylar sheets but pierced with 2 holes of radius R_t, located at $(x = \pm D_0, y = 0)$; iii) bronze sheets of thickness $h = 0.3$ mm, bending modulus $\kappa = 0.34$ N m and Poisson ratio $\nu = 0.3$.

Let us describe our first observations for each plate type. i) This is the reference case studied in [24]. If the centre of the sheet is displaced, two d-cones appear in symmetrical positions $(x = \pm D, y = 0)$, and move toward the clamped sides as Z is increased. Their distance D to the centre, their radius R and their tip angle ϕ are given by [24]

$$kD = kR = \sqrt{kZ}, \qquad \phi = 2\sqrt{kZ}/\mu, \tag{5}$$

at small Z, k being half the cylinder top curvature and $\mu = 4.8$ a geometrical factor. At large Z, other patterns occur, but are not useful to the present study. ii) With pierced mylar sheets, the observations are similar, but the d-cones tips are slightly attracted and pinned by the holes. The effect of the holes is felt over a distance of the order of their diameter $2R_t$. Energy is gained when the cone tip is in a hole and the core "suppressed", so that the pinning could be expected. iii) The first loading of bronze sheets is almost identical to the case i). A mylar sheet would show exactly the same patterns if reloaded. At the second loading of the bronze plate, the d-cones move faster toward the clamped sides; at a given Z, the d-cones can be up to 2 cm nearer to the sides than with a mylar sheet. The subsequent loadings are similar to the second loading. The simplest interpretation is that the material is "softened" at the first loading: It undergoes plastic deformations so that its equilibrium state is changed to a state nearer to the deformed state. Thus it is easier to deform it later on. We will discuss this point in the last section.

The elastic energy of the core. – We now use the results on pierced mylar sheets. The gain of energy at the pinning can be observed on the force/displacement curves $F(Z)$ (fig. 2):
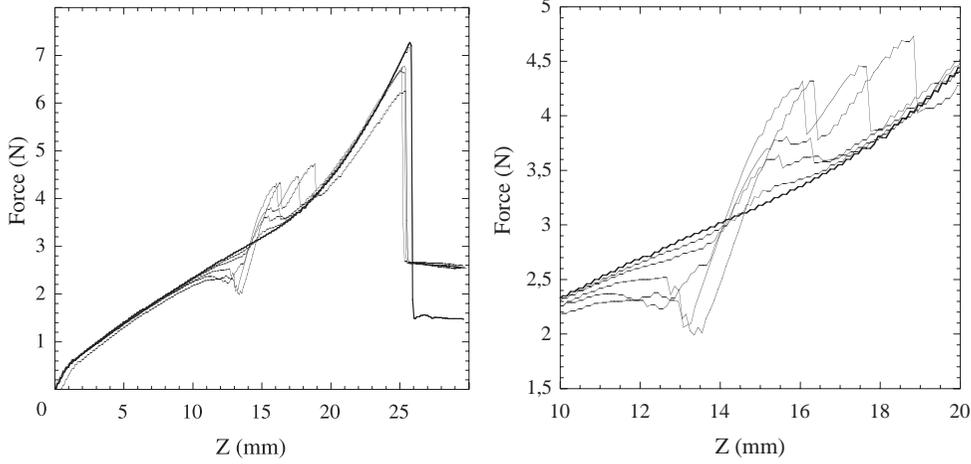
Fig. 2 – Pierced mylar sheets: Resisting force F vs. vertical displacement Z of the plate centre (left), for $\alpha = 30°$, $d = 21$ cm (see fig. 1) and a zoom (right). The distance between the holes is $2D_0 = 10$ cm and their radii range from 0 (thick line) to $R_t = 6$ mm (smaller to larger bumps). When the d-cones tips enter the holes, pierced sheets are easier to deform as energy is gained at the pinning. The two d-cones sometimes depin at different displacements Z, so that the force curve has two peaks at the depinning. When the d-cones are far from the holes the curves are identical as the holes are only a small perturbation.

the force decreases when the tip enters in the hole and reaches the same value as without a hole after the depinning. The gain of energy can be computed from the force integral $\int F(Z)\, dZ$; its maximal value $\Delta\mathcal{E}$ increases with the area of the holes. Each hole (radius $R_t \leq 6$ mm) is smaller than the d-cone core (radius $R_c \sim 10$ mm, as given by eqs. (3)-(5)). As a consequence, we expect the maximum energy gain $\Delta\mathcal{E}$ to occur when the d-cone tips are at the hole centres and to result from the suppression of a part of the core of radius R_t: this region has become virtual. Assuming that the elastic energy is evenly distributed in the core, and using eqs. (4)-(5), the energy of a disc of radius R_t in the core (half the gained energy) is found to be

$$\kappa\gamma G\phi^2 \left(R_t/R_c\right)^2 = 4\kappa\gamma Gk^2 D_0^2/\mu^2 \left(R_t/R_c\right)^2 = \Delta\mathcal{E}/2. \tag{6}$$

The factor 2 stands for the two d-cones. This equation allows the collapse of the experimental results on a single curve (fig. 3), and the fit gives a measurement of the core geometric factor,

$$\gamma = 0.53 \pm 0.04. \tag{7}$$

It is rather large as we expected γG of order one. Thus, we obtain the first measurement of the core energy.

To support this estimation, we minimized the elastic energy of the core,

$$\int \left(2\kappa M^2 + Eh/2(\Delta^{-1}K)^2\right) dr\, rd\theta. \tag{8}$$

M and K are the mean and the Gauss curvature, respectively, and Δ^{-1} is the inverse Laplacian. We assumed the shape of the cone to be given by a test function $\xi = R_c g(r/R_c)\psi(\theta)$, in polar coordinates (r, θ), g being a polynomial of degree 8. This shape has to be matched to the cone $\xi = r\psi(\theta)$, so that ψ is identical with the outer solution [18], and g and its two
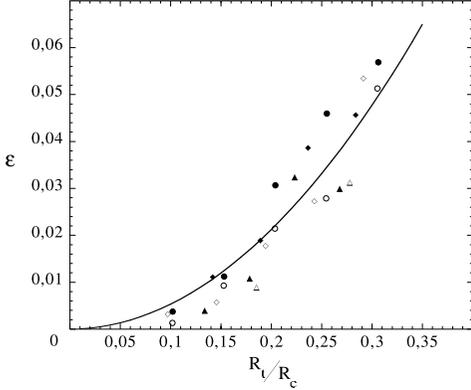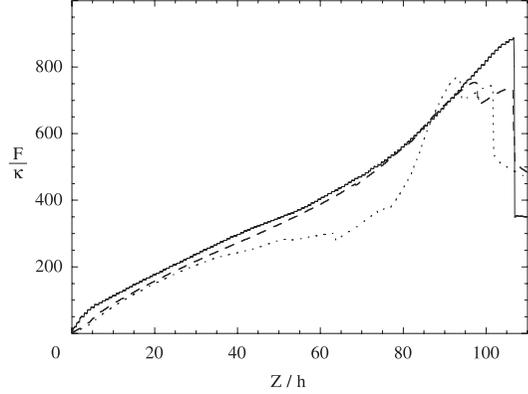
Fig. 3   Fig. 4

Fig. 3 – The core energy: non-dimensional maximum energy gain ϵ *vs.* the ratio of the hole radius to the d-cone core radius R_t/R_c, for various values of the geometrical parameters (α, d and D_0). The error on ϵ is constant ($\simeq 10^{-2}$). $\epsilon = \Delta\mathcal{E}\mu^2/(8\kappa G k^2 D_0^2)$, $\Delta\mathcal{E}$ being the maximum energy gain, μ and G geometrical parameters, κ the plate bending modulus, $2k$ its initial curvature and $2D_0$ the distance between the holes. Line: fit to $\epsilon = \gamma(R_t/R_c)^2$ (eq. (6)).

Fig. 4 – Plastic deformations: reduced force F/κ *vs.* non-dimensional displacement Z/h for: i) loading of an elastic mylar plate (solid line); ii) first loading of a bronze sheet (dashed line); iii) second loading of the same bronze sheet (dotted line). i) and ii) are identical except at large Z.

first derivatives are matched to r. This choice allows an analytical computation of the inverse Laplacian. The minimisation of the energy by varying the coefficients of the polynomial g leads to $\gamma = 1.05$. Of course, this is an upper bound, as we have not solved the Föppl-von Kármán equations exactly, but it has the right order of magnitude.

Plastic deformations in the core. – The first surprise came from the identity between the force curves for unpierced mylar sheets and bronze sheets loaded for the first time (fig. 4), although the bronze sheets undergo irreversible deformations. At the second loading of bronze sheets, the resisting force is smaller than at the first load. At the subsequent loadings, the force does not differ significantly from the second loading. Besides, it does not depend on the displacement velocity nor on the duration of the first loading (within experimental errors).

Most materials behave elastically below a critical strain a_0 (of the order of 1%, see [28]), and plastically above. The material has a residual strain (its length at equilibrium changes irreversibly) when the strain is decreased from above a_0: plasticity can be viewed as a memory of large deformations. To characterize the bronze sheets that we have used, we performed a separate experiment: we imposed their curvatures by folding them onto rigid cylinders of different radii. When released, the sheets had a residual curvature (they became curved at equilibrium) if the imposed curvature was large enough. As the maximum strain $a = hc/2$ is proportional to the sheet curvature c, we obtained an empirical law for the residual strain a_r as a function of the imposed strain a_i: we fitted

$$a_r = \beta(a_i - a_0)^2 H(a_i - a_0) \equiv f(a) \tag{9}$$

to the experimental data. H is the Heaviside function: there is a residual deformation only over the yield strain a_0. This fit gave $\beta = 128$ and $a_0 = 4.8 \cdot 10^{-3}$, which characterize the bronze used here. These quantities, as well as the law of eq. (9), are material dependent, but
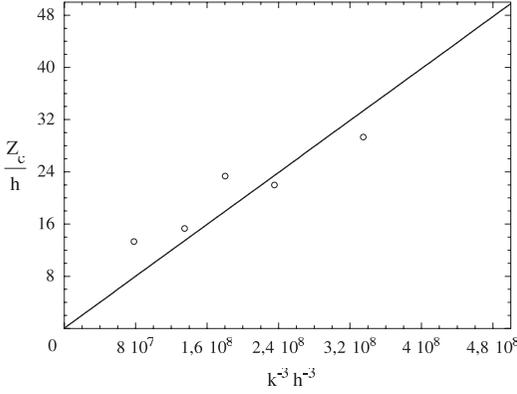
Fig. 5
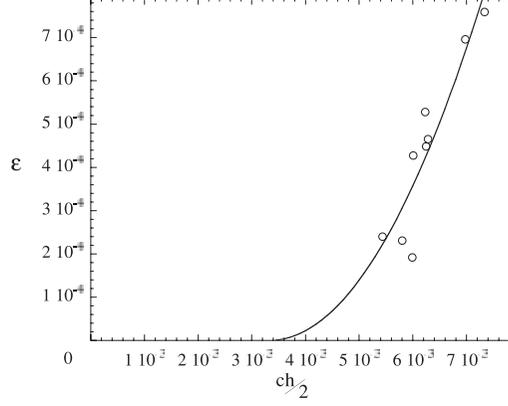
Fig. 6

Fig. 5 – The critical displacement leading to plastic deformations Z_c as a function of the curvature k, and fit to eq. (10) (h the sheet thickness). The error on Z_c/h is constant ($\simeq 7$).

Fig. 6 – Plastic deformations: non-dimensional energy gain ϵ $vs.$ the strain in the core $ch/2$. $\epsilon = \Delta\mathcal{E}h\mu^2/(8\kappa GR_c^2 c)$ corresponds to the energy difference between the first and the second loading of a bronze sheet (same notations as in fig. 3 and c is the curvature in the core). Line: fit to eq. (11).

that should not affect the generality of the following analysis. Equation (9) is reasonable for so-called strain-hardening materials [28].

Figure 4 shows that, in fact, the second loading of bronze sheets differs from the first loading only above a critical displacement Z_0, which can be predicted as follows. The curvature in the cone is ϕ/r, r being the distance to its tip, so that the curvature in the core is $c = \phi/R_c$. Memory effects start when the strain in the core $\phi h/(2R_c)$ reaches the yield threshold a_0. Using eqs. (3), (5), we get the critical displacement for plastic deformations,

$$Z_c = \frac{\mu a_0^3}{\sqrt{48(1-\nu^2)}} \frac{1}{h^2 k^3}. \tag{10}$$

A fit to the data of fig. 5 leads to $a_0 = 5 \cdot 10^{-3}$, in agreement with the measured value $(4.8 \cdot 10^{-3})$.

Now we consider the difference in forces between the two first loadings. By integration, we obtain the difference in energies $\Delta\mathcal{E}$ between the loadings. We estimate $\Delta\mathcal{E}$ from the changes in the core. Using eqs. (3)-(5), the energy of the core at the first loading can be rewritten as $E_c = 2\gamma G\kappa c^2 R_c^2/\mu^2$. The equilibrium curvature becomes $c_r = 2\beta(ch/2-a_0)^2/h$ after the first loading (from eq. (9)). The energy of the plate at the second loading is obtained by replacing c by $c-c_r$ in E_c: $E_c^{(2)} = 2\gamma G\kappa(c-c_r)^2 R_c^2/\mu^2$. The difference $\Delta\mathcal{E} = E_c - E_c^{(2)}$ equals

$$\Delta\mathcal{E} = 8\kappa G\gamma R_c^2 \frac{c}{h\mu^2} f\left(\frac{ch}{2}\right); \tag{11}$$

f is the function defined in eq. (9). Using the measured core geometrical factor γ, the fit with the experimental data of fig. 6 leads to the material parameters $\beta = 94$ and $a_0 = 3.4 \cdot 10^{-3}$, slightly smaller than the measured values ($\beta = 128$ and $a_0 = 4.8 \cdot 10^{-3}$). Thus, we have modeled the loss of energy in the d-cone cores when irreversible deformations occur. This type of modeling would probably explain the singularity energy measured for a single d-cone [19].

Conclusion. – We have been able to measure the energy of the core for both elastic and plastic deformations. The first loading of a bronze sheet can be predicted from the usual elasticity theory; the second loading is well described with a model for the memory of deformations. These results show that all the recent works using linear elasticity can have a practical relevance. Further developments could stem from using our results in complex situations with a large number of singularities as for crumpled paper [29, 30].

<center>* * *</center>

REFERENCES

[1]   Yamaki N., *Elastic Stability of Circular Cylindrical Shells* (North-Holland) 1984.
[2]   Roman B. and Pocheau A., *Europhys. Lett.*, **46** (1999) 603.
[3]   Bourdieu L., Daillant J., Chatenay D., Braslau A. and Colson D., *Phys. Rev. Lett.*, **72** (1994) 1502.
[4]   Saint-Jalmes A. and Gallet F., *Eur. Phys. J. B*, **2** (1998) 489.
[5]   Helfer E., Harlepp S., Bourdieu L., Robert J., MacKintosh F. C. and Chatenay D., *Phys. Rev. Lett.*, **87** (2001) 088103.
[6]   Svoboda K., Schmidt C. F., Branton D. and Block S. M., *Biophys. J.*, **63** (1992) 784.
[7]   Nelson D., Piran T. and Weinberg S. (Editors), *Statistical Mechanics of Membranes and Surfaces*, Vol. **5** (World Scientific, Singapore) 1988.
[8]   Spector M. S., Naranjo E., Chiruvolu S. and Zasadzinski J. A., *Phys. Rev. Lett.*, **73** (1994) 2867.
[9]   Landau L. and Lifchitz E., *Théorie de l'élasticité* (Mir, Moscow) 1990.
[10] Seung H. S. and Nelson D. R., *Phys. Rev. A*, **38** (1988) 1005.
[11] Patrício P. and Krauth W., *Int. J. Mod. Phys. C*, **8** (1997) 427.
[12] Pogorelov A. V., *Bendings of Surfaces and Stability of Shells* (American Mathematical Society) 1988.
[13] Witten T. A. and Li H., *Europhys. Lett.*, **23** (1993) 51.
[14] Lobkovsky A. E., Gentges S., Li H., Morse D. and Witten T. A., *Science*, **270** (1995) 1482.
[15] Pomeau Y., *C. R. Acad. Sci. Paris Sér. I*, **320** (1995) 729.
[16] Ben Amar M. and Pomeau Y., *Proc. R. Soc. London, Ser. A*, **453** (1997) 729.
[17] Chaïeb S., Melo F. and Géminard J.-C., *Phys. Rev. Lett.*, **80** (1998) 2354.
[18] Cerda E. and Mahadevan L., *Phys. Rev. Lett.*, **80** (1998) 2358.
[19] Chaïeb S. and Melo F., *Phys. Rev. E*, **60** (1999) 6091
[20] Cerda E., Chaïeb S., Melo F. and Mahadevan L., *Nature*, **401** (1999) 46.
[21] DiDonna B. A., Venkataramani S. C., Witten T. A. and Kramer E. M., *Phys. Rev. E*, **65** (2002) 016603.
[22] Pauchard L. and Rica S., *Philos. Mag. B*, **78** (1998) 225.
[23] DiDonna B. A. and Witten T. A., *Phys. Rev. Lett.*, **87** (2001) 206105.
[24] Boudaoud A., Patrício P., Couder Y. and Ben Amar M., *Nature*, **407** (2000) 718.
[25] Kléman M., *J. Phys. (Paris)*, **41** (1980) 737.
[26] Amirbayat J. and Hearle J. W. S., *Int. J. Mech. Sci.*, **28** (1986) 339.
[27] Boudaoud A. and Chaïeb S., *Phys. Rev. E*, **64** (2001) 050601(R).
[28] Johnson W. and Mellor P. B., *Engineering Plasticity* (Ellis Horwood Limited) 1983.
[29] Plouraboué F. and Roux S., *Physica A*, **227** (1996) 173.
[30] Matan K., Williams R., Witten T. A. and Nagel S. R., *Phys. Rev. Lett.*, **88** (2002) 076101.